3D ultrasound characterization of woven composites

Rostand B. Tayong, Martin J. Mienczakowski, and Robert A. Smith

Citation: AIP Conference Proceedings **1949**, 130008 (2018); doi: 10.1063/1.5031603
View online: https://doi.org/10.1063/1.5031603
View Table of Contents: http://aip.scitation.org/toc/apc/1949/1
Published by the American Institute of Physics

3D Ultrasound Characterization of Woven Composites

Rostand B. Tayong[a)], Martin J. Mienczakowski[b)] and Robert A. Smith[c)]

Department of Mechanical Engineering, University of Bristol, University Walk, Bristol BS8 1TR, United Kingdom.

[a)]Corresponding author: rt14172@bristol.ac.uk
[b)]martin.mienczakowski@bristol.ac.uk; [c)]robert.smith@bristol.ac.uk

Abstract. Recent studies on the Non-Destructive Testing (NDT) of composites for the aerospace industry have led to an understanding of ultrasonic propagation in these materials [1]. Techniques for enhanced ultrasonic imaging of the internal structure of composite laminates containing unidirectional fibers have been proposed and tested in a laboratory environment. For the automotive industry, textile composites are often preferred and widely used. The reason for this is that these types of composites offer good mechanical performance, with resistance to delamination and reduced manufacturing costs. In this study, two models are developed and shown to be suitable to characterize the woven specimen. The first model is a 1D analytical model that makes simplified assumptions and the second is a 3D time-domain Finite Element (FE) model developed [2] for advanced understanding of the woven composite response to an ultrasonic excitation. For each of the proposed models, three parameters are defined and used to analyze the structure behavior. They are the instantaneous amplitude, instantaneous phase and instantaneous frequency. These parameters are employed to track the in-plane fiber orientation and the ply-interface location and for the sentencing of features. Three different specimens with the following weave type: 3D orthogonal, 2D plain and Multilayer stitching were considered and scanned (using a focused ultrasonic transducer) to validate the proposed models. As a preliminary study, the work only focuses on the Orthogonal weave specimen. The results obtained from experimental, analytical and FE modeling, B-scan and C-scan are compared, discussed and presented in terms of the above defined parameters.

INTRODUCTION

There is a fast growing interest for textile composites in the automotive, aerospace and manufacturing industries. In principle, textiles are made from interlocked, interlaced (woven composites) or knitted yarns that undulate above and on top of other yarns in a well-defined way to form a single complex architecture. These types of composites are known to offer many possible architectures with high ratios of strain to failure in tension, compression or impact load when compared to classical unidirectional composite materials [3].

Woven composites are created by interlacing the wefts (continuous fibers arranged in the filling direction also known as the 0° orientation) and the warps (continuous fibers arranged following the 90° orientation) before impregnating the dry pre-form with a matrix (which is polymer resin for the presented study). The yarns (both weft and warp) are often arranged following an intelligent pattern or weave style that gives its name to the woven fabric. Woven composites can be classified in two categories: 2D and 3D woven composites. In 2D woven fabrics, a warp yarn weaves above and below only one set of weft yarns to produce a sinusoidal (regular and periodic) longitudinal profile. Some well-known examples are plain, satin and twill weaves. The 3D woven composites are designed with the aim to reinforce the third dimension in order to reduce the potential for delamination between the layers. Some examples are Orthogonal, multilayer stitching and angle-interlock weaves. Early works on modeling woven composites, such as the work by Pierce [4], suggested the consideration of yarns of circular cross-section to simplify the woven composite's geometry and therefore the response to any mechanical excitation. The suggested assumption is described to be efficient for large (semi-infinite or infinite) material sizes when subjected to relatively small excitation amplitudes. Later on, models with refined geometries [5, 6] for the yarns were proposed and contributed to the understanding of the mechanical behavior of woven composites. Naik and Ganesh [7] proposed a simplified 2D analytical method to predict the thermo-elastic properties of plain-weave fabric laminates. Despite the fact that their method assumed non-twisted fibers, a relatively good agreement was obtained between the model and the experiment. It is worth noting that most of the published works on modeling woven composite are focused on the mechanical behavior; there are few studies focusing on the ultrasound response for this particular type of composite material. Despite the extensive work that has been carried out on ultrasound characterization of unidirectional plies [1, 8, 9], there is a need to investigate the application of the proposed methods to woven fabric laminates. Recent

44th Annual Review of Progress in Quantitative Nondestructive Evaluation, Volume 37
AIP Conf. Proc. 1949, 130008-1–130008-11; https://doi.org/10.1063/1.5031603
Published by AIP Publishing. 978-0-7354-1644-4/$30.00

advanced work from researchers at the University of Bristol suggest interesting potential for characterizing these fabrics using ultrasound methods. In particular, works by Smith et al. [10] on ultrasound characterization of composite materials (mainly aerospace unidirectional plies) have shown that in-plane fiber orientation, ply or layer interface location and other features can be analyzed in a successful way using instantaneous parameters of amplitude, phase and frequency. Various models [8, 11, 12, 13] of wave propagation across multi-layered systems such as composite materials were proposed, some based on analytical approaches such as the recursive [8] or transfer-matrix [12, 13] methods. These models are very often shown to be good enough to predict multi-layered systems' reflection or transmission coefficients. In most cases, the approaches assume simple configurations such as simple material shape cross-sections, isotropic effective media and mixture rules to account for the fiber in the resin and only consider normal-incidence plane-wave propagation [14]. A level of complexity is added when focused ultrasound fields, realistic defects [14] or complex-shape cross-sections are considered. This is when 2D and 3D numerical approaches are proven to be advantageous to understand the composites response or behavior. Recent advances in Finite Element (FE) methods make it possible to investigate with good precision local areas within the sample. Because woven composites have a complex architecture, their geometries are often built thanks to dedicated software like TexGen [15]. TexGen is an open source software developed at the University of Nottingham for the modeling of textiles geometry. This software works both under a Graphical User Interface (GUI) or a Python code script that makes it possible to create the different weave stitching. Once the geometry is built, it can be exported to the FE code via a Matlab code [16] that processes to create a native PZFlex voxel format file with the desired simulation settings for the ultrasound simulation. PZFlex is the FE code used to run the ultrasound simulation for this work. FE models for woven textiles are often carried out and presented as assemblages of unit cells also known as representative unit cells [3]. The unit cell is a repeating cell obtained from the weave fabric and is very important because it helps to reduce the complexity and size of the model.

The presented work investigates the 3D ultrasound characterization of woven composites. A particular emphasis is given to the Orthogonal weave type at a frequency that excites the different internal resonances. Two models are presented in this work as described above - a 1D analytical model and a 3D FE model. Results from both models are compared with experimental data. The presented work is structured as follows. The next section deals with the analytic-signal formulation and instantaneous-parameters definition. Next, the experiment setup is presented and some interesting initial analyses are discussed. Later on the modeling (analytical and numerical) is described and benchmarked against the real data in the results and discussion section. The important results obtained for the presented work are summarized in the conclusion.

ANALYTIC SIGNAL FORMULATION AND INSTANTANEOUS PARAMETERS

The ultrasound propagation of waves within a structure can be described by the following complex expression

$$x(t) = A(t)e^{i\rho(t)} \tag{1}$$

where $x(t)$ is the analytical signal, $A(t)$ is the instantaneous amplitude and $\rho(t)$ is the instantaneous phase. Very often in Acoustics, only one property such as acoustic pressure or particle velocity is measured and this is the real part of the analytic signal [10]. In a complex plane, the analytic-signal response is shown to go round a loop [10]. For a unidirectional ply, this loop is observed traverse a phase of 2π every ply. The characteristic of the laminate is that the phase is locked to those plies [10]. Woven fabrics are made of yarns rather than plies, so the resonances are more complex and change significantly from one location to the next. How similar physics can be applied to these materials is worth investigating and is described throughout this work. The instantaneous amplitude is the envelope of the signal and the phase represents how far around the complex loop in time the signal has progressed. The information about how rapidly the phase is changing with time is given by the instantaneous frequency $f(t)$ defined as the rate of change of phase with respect to time and is given by

$$f(t) = \frac{1}{2\pi}\frac{\partial \rho}{\partial t} \tag{2}$$

As will be shown in the results, instantaneous frequency is useful for characterizing the disturbances within the composite structure. It is expected that all three instantaneous parameters would contribute to a better analysis of in-plane fiber orientation (mainly the instantaneous amplitude), ply orientation or layer interface location (mainly the instantaneous phase) and particular features such as binder yarn effects (mainly the instantaneous frequency).

EXPERIMENTAL SETUP

Specimen Characteristics and Measurement

Initially, three different woven specimens of 1.7 mm thickness made of five layers each were scanned for this work. Those specimens are composed of 2D plain weave, 3D multilayer double-stitch and Orthogonal plain weave. For reason of simplicity, only the study for the Orthogonal plain weave fabric is presented in this work. This particular type of weave contains interesting features useful to understand the ultrasound response of the two other weave types. The characteristics of the different media used in the work are given in Table 1. The yarns for the specimens are made of carbon-fiber with thickness of about 0.19 mm suggesting a resonant frequency of 7.8 MHz. The fibers have a diameter of 7 µm. Figure 1 depicts the studied specimen showing the weave stitching (Fig. 1a), the real specimen top view taken with a microscope (Fig. 1b), the TexGen generated geometry (Fig. 1c) and the geometry showing the defined local number of yarns (Fig. 1d). One can observe from Fig. 1b that, due to the specific stitching, the rows denoted 5050505 do not appear to be present. Therefore, the study will focus on investigating the ultrasound responses for regions denoted 6161616 (which correspond to slices along the binder yarn) and 9494949 (which correspond to slices of five layers of 0° orientation and four layers of 90° orientation separated by just four layers of 90° orientation).

TABLE 1. Default materials properties used for the woven specimens modeling. The Fiber Volume Fraction is considered to be 60%. Other information about the studied specimen can be found in [17].

	Density (kg/m^3)	Longitudinal velocity (m/s)	Shear velocity (m/s)	Attenuation (dB/mm/MHz)
Water	998.2	1433.07	-	-
Epoxy resin	1270	2902.62	2052.46	0.15
Yarns	1690	2832.27	1332.20	-

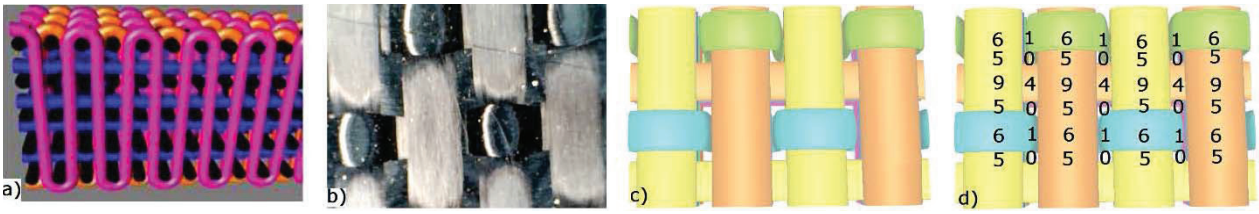

FIGURE 1. Orthogonal weave specimen: a) Weave stitching; b) Real specimen top view taken with microscope; c) TexGen generated geometry; d) TexGen generated geometry showing the local number of yarns. Further info in [17].

An ultrasonic immersion scanning method is used for the experimental setup. To scan the specimen, a 3-axis scanning system provided by Ultrasonics Sciences Limited was used. The specimen was ensured to be as flat as possible during the scanning process. A Pulse-Echo method was used to acquire the data and the obtained signal, after scanning with a 0.2 mm pitch, was recorded during a continuous raster scan. Three focused (1.5 inch spherical) ultrasonic transducers were used: 5 MHz, 7.5 MHz and 10 MHz. The presented work focuses on the results obtained at 5 MHz in order to explain the phenomena by exciting the different internal regions resonances. A future study is planned to describe and compare the obtained results for the other frequencies and specimens.

Initial Analytic-Signal Analysis

Figure 2 presents the experimental B-scan results for the RF waveform along the two different slices. In Fig. 2a, the result on the region denoted 94949 (region where the 90° weft-yarns separate the warp-yarns) is shown. For this region, as described earlier, there is an alternating number of 9 and 4 yarns. The ultrasound waves therefore have to propagate through areas where the Fiber Volume Fraction is higher (around 60%) and lower (around 30%). This respectively causes a higher and lower velocity across the specimen. The direct consequence of this velocity change is a variation in the time of arrival of each resin inter-layer reflection, including the back wall echo, creating the

observed undulations. This result suggests that the ultrasound response is affected by the specimen weave. Each weave type is expected to have a characteristic periodic response which is directly linked to the weaving of the yarns. This suggests the possibility of considering a weave signature to assist in analyzing the weave structure. In order to apply the ultrasound techniques necessary to investigate the internal structure of the woven fabric, a correction to the acoustic velocity variation is needed, based on flattening the back-wall reflection across the scan. This correction should be applied only if the back wall is known to be flat and perpendicular to the wave propagation. The suggested correction is carried out as shown in Fig. 2b where the undulations are flattened out at the back-wall location. In Fig. 2c the cross-section result for the region along the binder yarn (region denoted 61616) is shown. For this region, the wave propagates across both locations of 6 yarns (5 wefts + 1 binder yarn) and 1 yarn (vertically oriented binder yarn). For this 1 yarn region the higher stiffness direction of the fiber is vertical and aligned to the direction the ultrasound wave propagates, causing no reflection from this location. The reason for this is presumably due to the fact that in this location, the yarn acts like a waveguide with very high velocity and therefore, part of the wave energy would travel along the yarn.

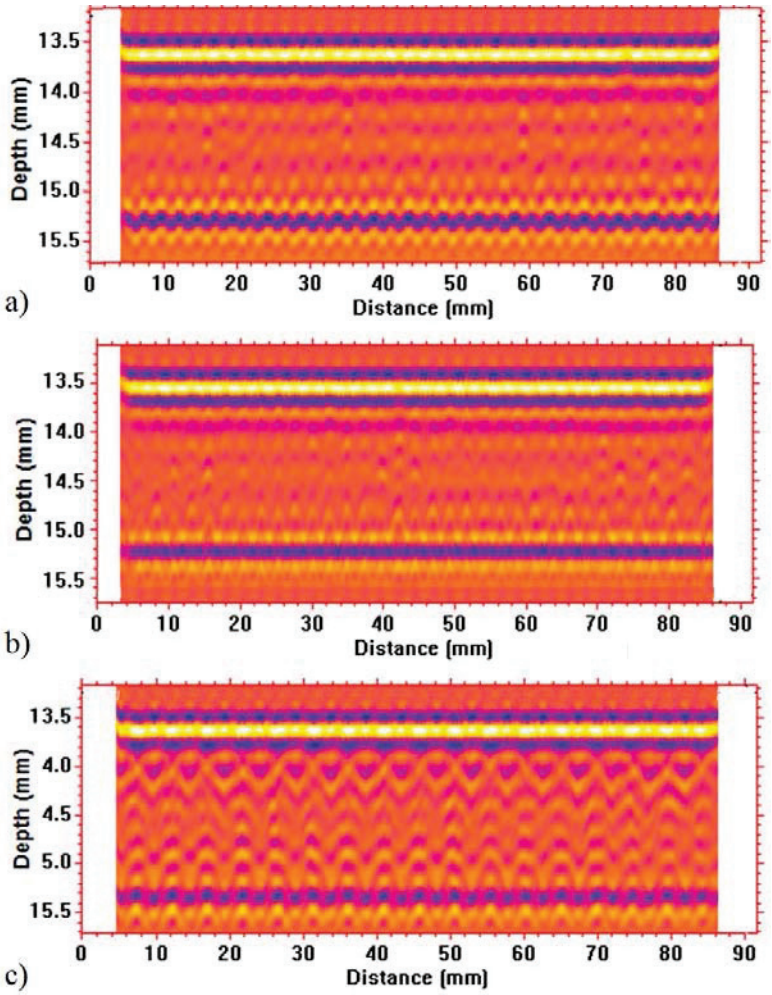

FIGURE 2. Orthogonal weave specimen. RF waveform experimental results for slices along a) the 94949 location without the velocity correction, b) the 94949 location with the velocity correction, and c) the 61616 region known as the binder yarn region.

Figure 3 shows the experimental in-plane C-scan results taken at 0.1 mm depth below the front surface and showing the three instantaneous parameters. The level of gray scale for the instantaneous amplitude (Fig. 3a) reveals the weave signature where the binder-yarn regions (square high-amplitudes) are surrounded by weft region (tall rectangular high-amplitude regions). Although it is less clear, a similar observation is made for the instantaneous-phase result (Fig. 3b). Regions in red alternate with regions in light blue and the regions of change of phase are noticeable. The instantaneous-frequency result shown in Fig. 3c is very interesting as it clearly reveals regions of

high and low frequency, indicative of reduced and increased yarns spacing, respectively. The regions of higher frequency (in red) can be associated with the binder yarns going on top of a set of weft yarns. Since the binder yarn squashes the yarns beneath, this results in a decrease of the yarn spacing through a reduction in the resin layer thicknesses between yarns. Where the binder yarn goes beneath the wefts, the same effect happens at depths close to the back wall. It is also observed on these C-scan results that the binder-yarn locations at a depth near the front or back surfaces, are arranged in a hexagonal pattern, the exact shape of which is determined by the relative warp and weft yarn widths. The capacity for revealing such changes or features in the woven specimen is essential in order to characterize its response and to reveal any defect or deviation from design occurring in the sample.

ANALYTICAL MODELING OF PLANE-WAVE PROPAGATION IN A 3D WOVEN COMPOSITE

The presented analytical model is based on the recursive approach applied to multi-layer systems. This model assumes normal incidence of a propagating plane wave. A mixture rule for fibers in resin is considered following the Hashin [18, 19, 20] method. The described 1D analytical model [8] was initially benchmarked against a numerical [21], other analytical [13] models and experiment. Detailed description for this model can be found in various published works [8, 14]. Therefore, this section will focus only on presenting configurations relevant to the studied textile composites. Figure 4 depicts the schematic approach of modeling the slice across the binder yarn location using the recursive model by plotting side-by-side numerous 1D model results with different layer thicknesses in each case.

One can observe that this binder-yarn region is composed of three sub-regions depending on the number of yarns and resin-layer arrangements (a similar schematic can be done for the other slice region denoted 94949). The model can be used to map the reflection coefficient at any location across the considered sub-region. The obtained reflected coefficient is convolved with realistic input pulse using a Gaussian spectrum with controllable-center frequency and -6 dB bandwidth and a uniform phase (with frequency) defining the phase at the peak of the input-pulse envelope.

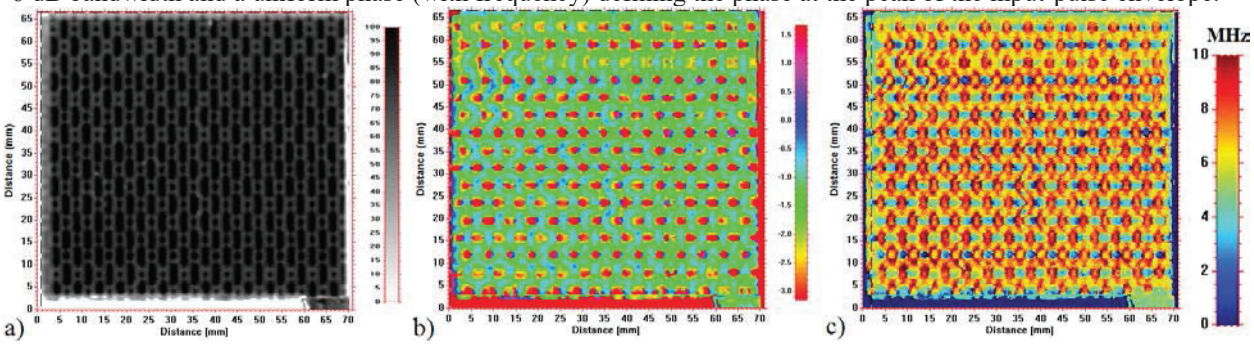

FIGURE 3. Orthogonal weave specimen. C-scan experimental results taken at 0.1 mm below the front surface. a) Instantaneous amplitude. b) Instantaneous phase. c) Instantaneous frequency.

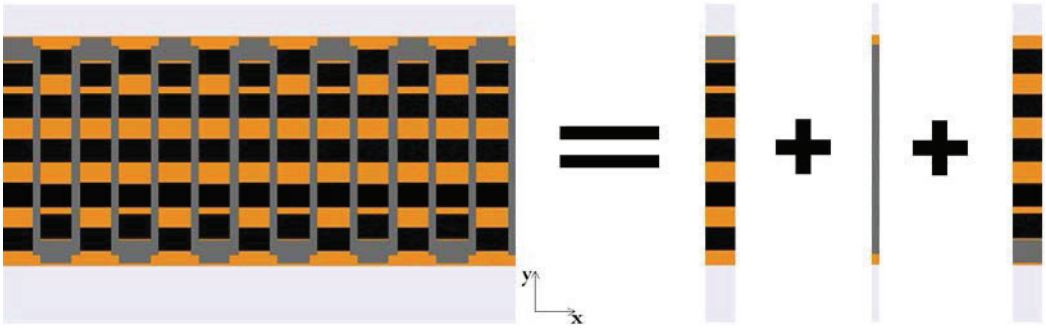

FIGURE 4. Principle of the recursive modeling applied to a slice along the binder yarn location for the Orthogonal weave composite. The figure on the left is a combination of the 1D models on the right hand side. The light gray regions represent the embedding medium, which is water for this study; the darker gray regions show the binder yarn; the light brown color is used to represent the resin layer regions whereas the black regions depict the weft region. The plane wave is assumed propagating in the direction vertically downwards.

NUMERICAL MODELING OF THE ULTRASOUND PROPAGATION IN A 3D WOVEN COMPOSITE

Among the numerical methods that exist, Finite Element (FE) analysis methods are known to be efficient to simulate the wave propagation through complex composite components. In this work, an FE model was developed to achieve this goal using the commercial time-domain FE package PZFlex. The geometry and the weave stitching are created using TexGen [15] which is a software package developed for modeling the geometry of textile structures by the University of Nottingham. In principle, the geometry created with TexGen is exported as a voxel file containing information about the yarn characteristics (orientation, number of layers and dimensions). The file is then processed to create a native PZFlex voxel format file with the desired simulation settings (central frequency of probe, bandwidth, angle of propagation, embedding medium, total runtime, type of yarn and matrix, Fiber Volume Fraction and the number of layers within the specimen). The technique for processing the generated voxel file is a bespoke in-house software developed in collaboration with the University of Strathclyde and PZFlex [16].

Assumptions and General Setting

A finite-size transmitting and receiving transducer of a square shape having 2.6 mm x 2.6 mm section is modeled with a water stand-off distance of 5.6 mm because this matches in focal plane and strength of focus (F number) - the focused immersion probe used in the experiments - it gives a natural focus (last axial maximum) in the middle of the sample. This modeled transducer moves on the model surface with a scan pitch of 0.2 mm - similar to the experimental one. Absorbing boundary conditions are used on the sides of the model and on the top surface except where it is in contact with the transducer. The ultrasound waves propagate along the z-axis in the negative direction as shown in Fig. 5. Twenty elements per wavelength per layer are considered for the modeled sample in order to allow a good accuracy and stability to ensure that any stress gradients are properly recreated. An impedance boundary condition is used at the bottom of the model removing the need to mesh the water beneath the model geometry. The use of such a boundary condition results in a considerable reduction of the total number of elements while providing the same accuracy and model stability and allowing the possibility to study larger dimensions of models. A total number of about 7 million elements was obtained for the specimen simulation suggesting a runtime of about half an hour on a desktop computer.

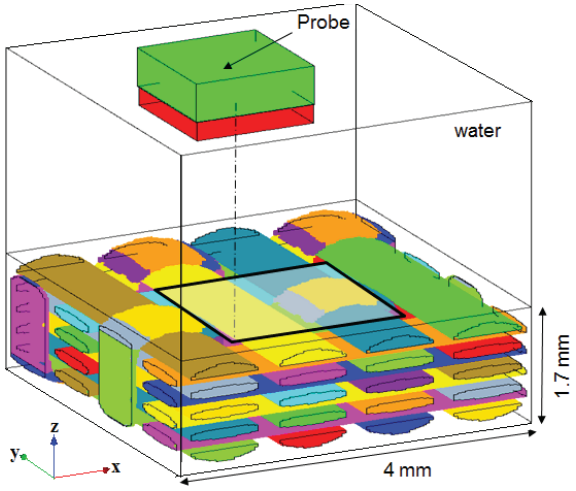

FIGURE 5. FE model geometry setup showing the imported Orthogonal woven specimen with the yarns of different colors and the planar transducer.

The complex nature of the woven fabrics and of the presence of the alternating regions with different numbers and densities of yarns, the fiber volume fraction and hence acoustic velocity is highly variable but periodic in nature. As for the experimental results, a correction is needed to compensate for these acoustic velocity variations assuming uniform velocity through the thickness, based on the time of flight to the peak in the back-surface signal. This correction is applied only if the internal structure investigations are needed and if the back surface is known to be

flat. Because of the periodic structure of the modeled geometry, only a minimum unique cell is numerically scanned by incrementing the probe position between model iterations. Considering the type of weave, a tessellation algorithm is applied to populate the result to a larger size of the specimen. The unit cell is considered to have orthotropic and homogeneous properties. The stiffness matrix calculation across the specimen is given as described in [22] in the following form:

$$\{C_{ij}\} = \begin{pmatrix} C_{11} & C_{12} & C_{13} & 0 & 0 & 0 \\ C_{12} & C_{22} & C_{23} & 0 & 0 & 0 \\ C_{13} & C_{23} & C_{33} & 0 & 0 & 0 \\ 0 & 0 & 0 & C_{44} & 0 & 0 \\ 0 & 0 & 0 & 0 & C_{55} & 0 \\ 0 & 0 & 0 & 0 & 0 & C_{66} \end{pmatrix} \quad 3)$$

Where C_{ij} represents the stiffness matrix coefficients obtained using the Young's and shear moduli and the Poisson ratios in the x, y and z directions and yz planes. These coefficients can be calculated using the material properties given in Table 1.

Transducer Focusing

Sound beams emitted by plane-piston ultrasonic transducer depict a characteristic known as natural focusing - the last axial maximum in the interference pattern is known as the natural focus. For a square plane piston, the near-field distance n where the natural focusing occurs is given by [23] as

$$n = 1.37\frac{d^2}{4\lambda} \quad 4)$$

Where d represents the square plane-piston width and λ is the wavelength. In practice, immersion transducers can be designed to have a controlled focus by shaping their surface. Figure 6a shows a descriptive scheme where the focal length of a transducer is set to occur at the middle of the composite sample. The advantage of focusing a beam is to concentrate the sound-wave energy to a specific region so as to increase sensitivity to small material changes in this region. For the presented work, the specimen was scanned with a spherical 1.5-inch transducer. The Finite Element model considers natural focusing defined to match the real transducer's focal plane and F number, as described in Fig. 6b. The distance s at which the planar transducer should be placed to give the same F-number as the experimental transducer is given by

$$s = \frac{dF}{D} \quad 5)$$

where F is the focal length of the experimental transducer in water and D is the transducer diameter. Figure 6b presents the effective water distance as a function of the element size. It also shows the unique point at which the natural focusing matches the experimental probe focusing (red circle). This result therefore suggests the use of a probe of 2.6 mm width and an effective water distance of about 8 mm, which translates to a water stand-off of 5.6 mm for a composite of thickness 2.4 mm. The choice of this point is expected to match the beam geometry of the experimental data.

RESULTS AND DISCUSSION

Figure 7 shows the C-scan instantaneous amplitude results comparing the FE model and the experimental results (depth of 0.1 mm below the front wall). This figure also shows the real specimen weave photograph taken with a VMS-004 microscope with 400x magnification and revealing the weave characteristic. At the chosen C-scan depth, the characteristic weave of this orthogonal specimen is observed for both the experimental and FE model results. In Fig. 7b and c, the taller high-amplitude regions depict the binder yarns traveling above a set of weft yarns. As explained earlier, the taller high-amplitude regions surrounding the square ones represent the weft yarn. These results suggest the potential for the instantaneous parameters to reveal the changes that could occur within the woven composite and that they would be suitable to characterize some defects. Good agreement between the experimental and FE model results is observed.

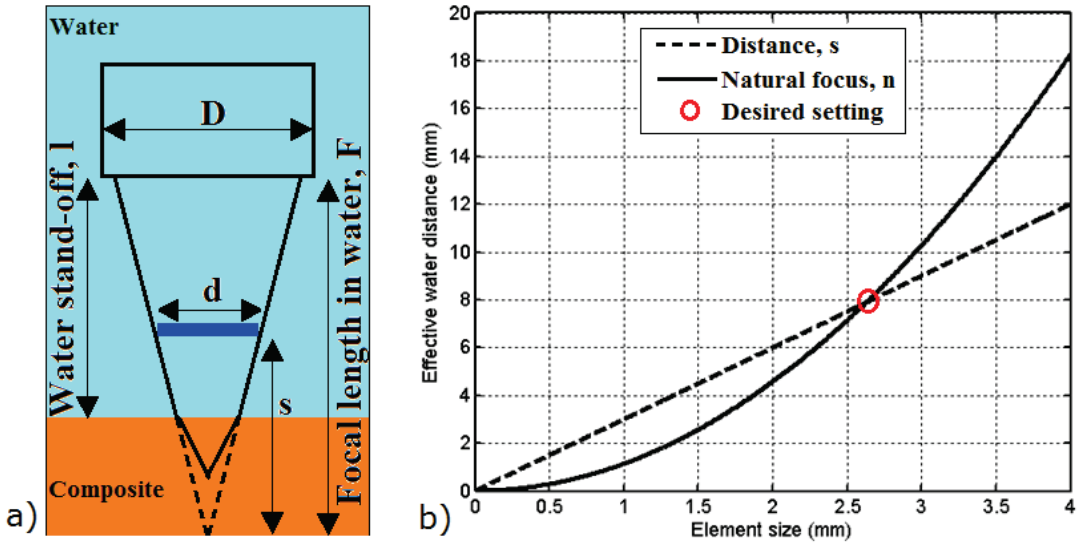

FIGURE 6. Transducer modeling. a) Description of the parameters used for the calculation. b) Effective water distances - to give the same F-number (dashed line) and distance to the natural focus (solid line), *n*, plotted against element size.

Figure 8 presents the instantaneous-frequency results comparing the analytical and FE models with the experimental results for a cross-sectional, B-scan slice cut along the binder yarn (61616 denoted region). The presented FE model accounts for the natural focusing of the planar probe. Alternating regions of high and low frequency are clearly observed. Near the front wall, the regions of high frequency can be linked to the binder yarn traveling on top of, and squashing, a set of weft yarns whereas near the back wall these regions are linked to the binder yarn traveling underneath a set of weft yarns.

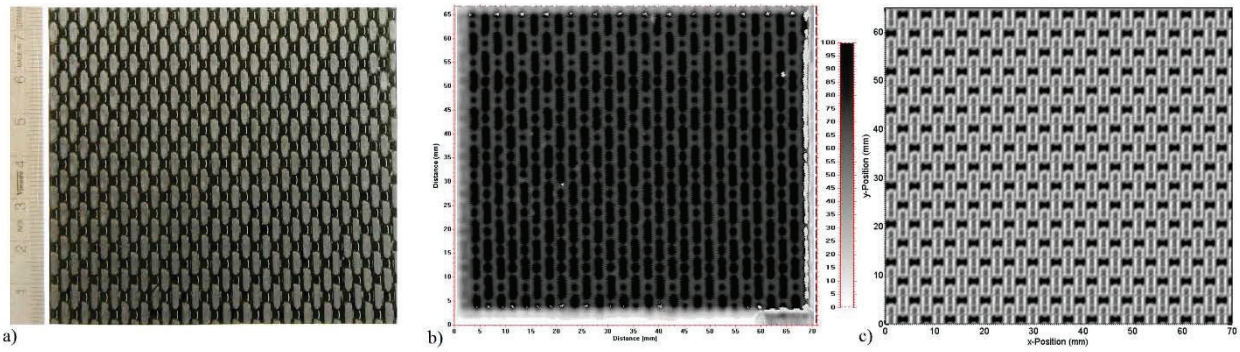

FIGURE 7. Orthogonal weave specimen picture and instantaneous amplitude results. a) Top view of the real specimen. b) Experimental result. Finite Element result. C-scan taken at a depth of 0.1 mm below the front wall.

In Fig. 8a, high frequency seems to split where a binder yarn is, presumably due to a squashing of several yarns and a crimping effect. In practice, due to the compaction of the yarns, the width of the weft yarns slightly varies across the specimen. This compaction would also normally create undulated vertical binder yarns across the specimen. The models (Fig. 8b and c) do not account for this compaction effect. Despite this difference, there is nevertheless a good agreement between the measurement and the models.

Figure 9 depicts the instantaneous frequency results comparing the analytical and FE models with the experimental results for a slice cut along the 91919 denoted region. As stated earlier, the FE model accounts for the natural focusing of the planar probe. From the experimental result (Fig. 9a), it is observed that high frequency seems to coincide with four in-page warp yarns between the five weft yarns. Good agreement is observed between the measurement and both the analytical and FE models.

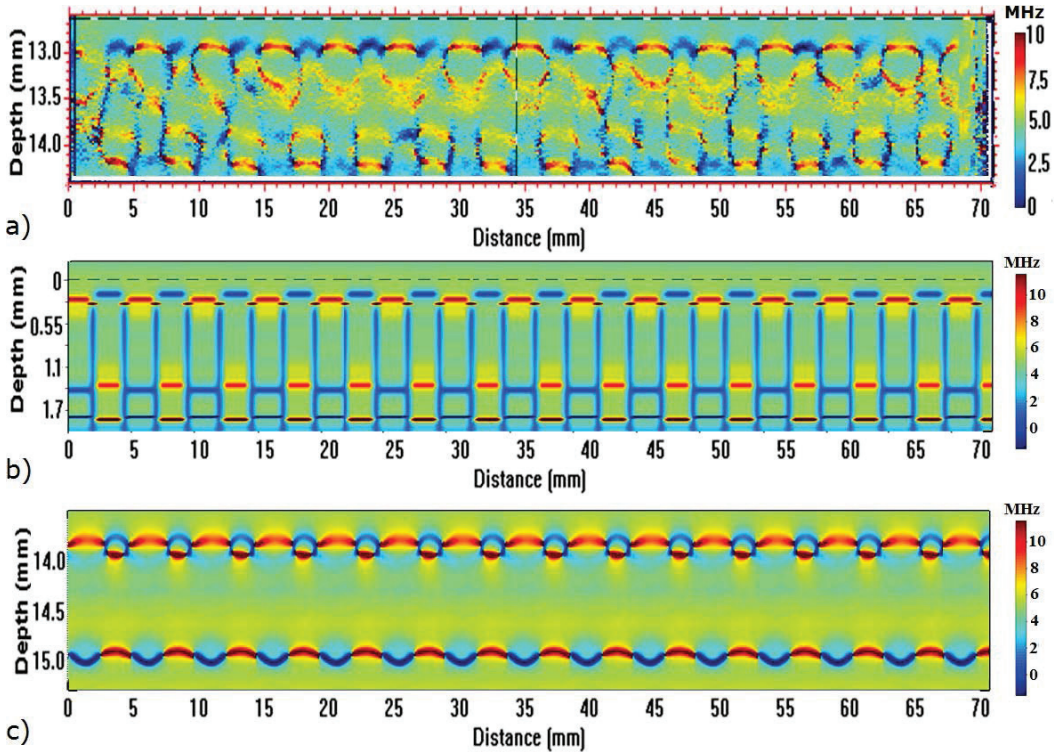

FIGURE 8. Orthogonal weave specimen results for the instantaneous frequency. a) Experimental data. b) Analytical model result. c) Finite Element result using natural focusing of the planar probe. This is a slice cut along the binder yarn (61616 region).

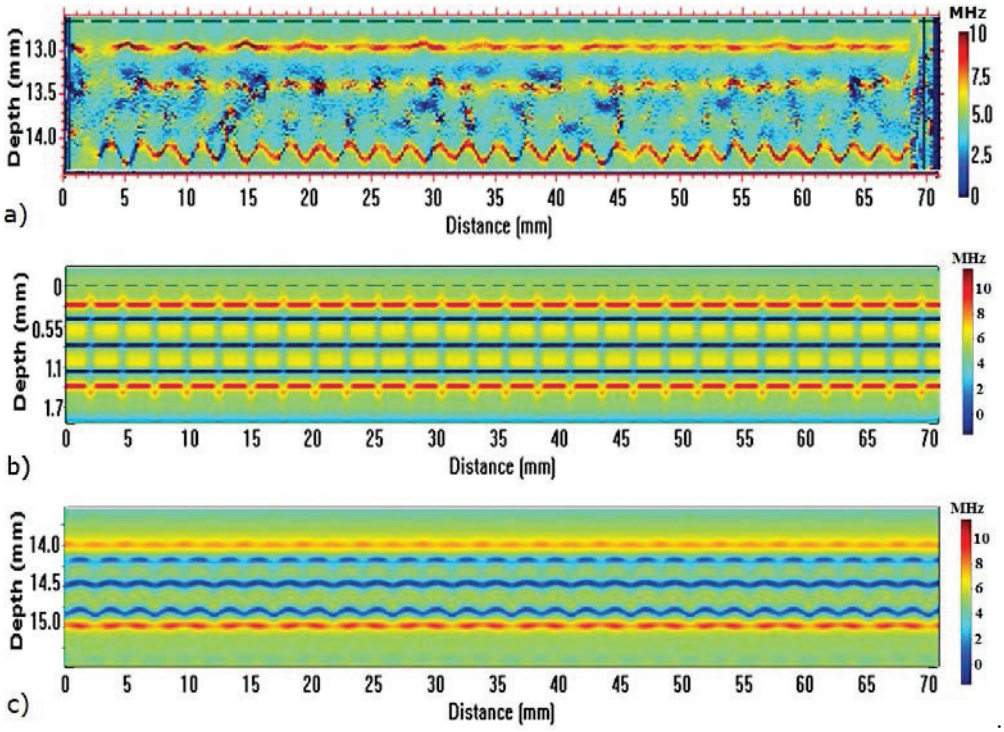

FIGURE 9. Orthogonal weave specimen results for the instantaneous frequency. a) Experimental data. b) Analytical model result. c) Finite Element result using natural focusing of the planar probe. This is a slice cut along the 91919 region.

CONCLUSION

The presented work dealt with a 3D ultrasound characterization of woven composites, particularly the Orthogonal weave type fabric. This woven specimen was tested using an ultrasonic immersion method. Both 1D analytical and 3D numerical models were developed and compared against the experimental results to understand the response and behavior of this woven fabric when subjected to an ultrasound excitation. For these models, three instantaneous parameters were defined and shown to be relevant in picking up the velocity changes with the Fiber Volume Fraction (FVF). The following remarks can be noted for the presented work:

- The orthogonal weave specimens depict 9 different regions with different FVF that result in a velocity variation across the woven composite. It is particularly shown that regions where the binder yarn is vertical and parallel to the ultrasound wave propagation present a characteristic for which no signal is received back to the transducer from the back surface.
- Periodic velocity variations across the 3D woven composite are large. The velocity variations can be corrected in order to apply the described ultrasound characterization methods.
- Three instantaneous parameters: instantaneous amplitude, phase and frequency were applied and revealed a great potential for tracking yarns in the 3D woven composites.
- Experimental data was acquired with a circular shape cross-section transducer with 1.5-inch spherical focus, whereas the Finite Element model considered a square shaped cross-section probe with self-focusing. Careful calculation was done and presented to set the FE probe to match the effective water distance corresponding to the realistic configuration.
- Good agreement is obtained between the experimental and both the analytical and numerical models results. Modeling has shown the potential for the instantaneous phase and frequency to detect manufacturing errors such as missed binder stitches.

The next step for this work would be to apply the spherical focusing to the FE model and completely validate this model using experimental results for the other weave type specimens. This work suggests the potential for mapping changes or defects within 2D and 3D woven composites.

ACKNOWLEDGMENTS

The authors would like to thank Dr. Louise Brown, University of Nottingham, Dr. Andrew Tweedie and Jeff Dobson, PZFlex, for help creating the textile geometry and importing it to the Finite Element model, and Dr. Hassan El-Dessouky, Advanced Manufacturing Research Centre (AMRC), for providing specimens. This research is part of a Fellowship in Manufacturing funded by the UK Engineering and Physical Sciences Research Council (EPSRC). Data available at: https://doi.org/10.5523/bris.37slm1qs12lw62mufbpz6m6j0r.

REFERENCES

1. R. A. Smith, L. J. Nelson, M. J. Mienczakowski, and R. E. Challis, *Insight*, **51** (2), 82-87, (2009).
2. X. Zeng, L. P. Brown, A. Endruweit, M. Matveev, and A. C. Long, *Composites: Part A,* **56**,150-160, (2014).
3. A. Dixit, H. S. Mali, and R. K. Misra, *Procedia Engineering*, **68**, 352-358, (2013).
4. F. T. Pierce, J. Text. *Inst.* **28**, 45-97, (1937).
5. F. Robitaille, B. R. Clayton, A. C. Long, B. J. Souter, and C. D. Rudd, *Inst. Mech. Engrs Proceedings*, Pt L: J. Materials: Design and Applications, **213**, 69-84, (2000).
6. F. Robitaille, B. R. Clayton, A. C. Long, B. J. Souter, and C. D. Rudd, Inst. Mech. *EngrsProceedings*, Pt L: J. Materials: Design and Applications, **214**, 71-90, (2000).
7. N. K. Naik and V. K. Ganesh, Composites **26**, 281-289, (1995).
8. R. A. Smith, "Use of 3D ultrasound data sets to map the localised properties of fibre-reinforced composites," PhD. Thesis, University of Nottingham, (2010).
9. E. A. Birt and R. A. Smith, *Insight,* **46** (11), 681-686, (2004).
10. R. A. Smith, L. J. Nelson, M. J. Mienczakowski, and P. D. Wilcox, *AIP Conference Proceedings,* **1706**, (2016).
11. S. I. Rokhlin and L. Wang, *International Journal of Solids and Structures,* **39**, 5529-5545, (2002).
12. B. Hosten and M. Castaings, *J. Acoust. Soc. Am*. **94** (3), 1488-1495, (1993).

13. T. P. Pialucha, "The reflection coefficient from interface layers in NDT of adhesive joints," Thesis, Imperial College, London, (1992).
14. R. B. Tayong, R. A. Smith, and V. J. Pinfield, "Acoustic characterization of void distributions across carbon-fiber composite layers," Review of Progress in Quantitative Nondestructive Evaluation (Vol. 36) , *AIP Conference Proceedings,* **1706**(1), 120008 (2016).
15. M. Sherburn and A. C. Long, "TexGen open source project open online at: http://texgen.sourceforge.net," (2010).
16. J. Dobson, A. Gachagan, R. O'Leary, A. Tweedie, and G. Harvey, "Finite element analysis of ultrasonic CFRP laminate inspection," *55th Ann. British Conf of ND Testing,* (2016).
17. H. M. El-Dessouky, A. E. *Snape*, J. L. Turner, M. N. Saleh, H. Tew, and R. J. Scaife, *Proc. SAMPE*, Washington (2017).
18. Z. Hashin, *J. Mech. Phys. Solids,* **13**, 119-134, (1965).
19. Z. Hashin, *J. Appl. Mech*. **46**, 546-550 (1979).
20. Z. Hashin, J. Appl. Mech. **29**, 143-150 (1962).
21. M. J. Mienczakowski, A. K. Holmes, and R. E. Challis, "Modeling of ultrasonic wave propagation in composite airframe, Review of Progress in Qualitative Nondestructive Evaluation (Vol. 34), AIP Conference Proceedings, **975**, 995-1001 (2008).
22. R. M. Jones, "Macromechanical behaviour of a lamina," *Mechanics of composite materials*, p. 59, (1999).
23. J. Marini and J. Rivenez, *Ultrasonics,* **12**(6), 251-256, (1974).